JOURNAL OF SOLID STATE CHEMISTRY **137,** 12–18 (1998)
ARTICLE NO. SC977642

Cesium–Sodium Ion Exchange on Hydrated Molybdenum Bronze and Formation of New Cesium Molybdenum Bronze by a Low-Temperature Synthesis Route

Kazuo Eda,*,[1] Takeshi Miyazaki,* Fumikazu Hatayama,† Masahito Nakagawa,‡ and Noriyuki Sotani*

*Department of Chemistry, Faculty of Science, Kobe University, Nada-ku, Kobe 657, Japan; †Department of Biofunctional Chemistry, Faculty of Agriculture, Kobe University, Nada-ku, Kobe 657, Japan; and ‡Department of Material Science, Faculty of Science, Himeji Institute of Technology, Kamigori-cho, Akogun, Hyogo 678-12, Japan

Received May 12, 1997; in revised form October 1, 1997; accepted October 13, 1997

The cesium-sodium ion exchange on the hydrated molybdenum bronze was investigated, and the proton in the intralayer site was found to prevent the complete ion-exchange of Cs/Na. The hydrated bronze of Cs with a larger ionic radius showed hydration behavior different than the bronzes of other alkali metals. Furthermore, the low-temperature synthesis route from hydrated molybdenum bronzes to alkali-metal molybdenum bronzes was investigated, and it was found that the route led to the formation of a new Cs molybdenum bronze, which was related to the family of blue alkali-metal molybdenum bronze $A_{0.3}MoO_3$. The lattice constants of the bronze were $a = 19.362(8)$, $b = 7.567(2)$, and $c = 10.506(4)$ Å, and $\beta = 121.07(3)^\circ$ (monoclinic system).

INTRODUCTION

Hydrated molybdenum bronzes are intercalation compounds of layered molybdenum trioxide. Such compounds have been expected to be interesting catalysts with special reaction fields and/or ion conductors. For such applications, it has been desired that a variety of ions can be intercalated into the host material, although so far only specific ions (i.e., alkali-metal ions, alkaline-earth metal ions, and a few transition-metal ions) have been intercalated (1–3). It has been known that large ions are not directly intercalated, and the ion-exchange technique is used for the preparation of intercalation compounds of such ions (1). In order to enable a variety of ions to be intercalated, it is important to reveal the factors which control the ion-exchange behavior on the hydrated bronze, so we have been studying the ion-exchange behavior over the past few years (4–6). And, in the present work, we investigated the ion exchange of Cs/Na.

[1] To whom correspondence should be addressed.

Furthermore, we have proposed that the hydrated bronze becomes an effective starting material for preparation of alkali metal molybdenum bronzes, which exhibit interesting low-dimensional electronic properties, among others (5–9). The alkali metal bronzes are formed from the hydrated bronzes at temperatures about 200 K lower than the formation temperature of the usual preparation methods (using A_2MoO_4–MoO_3 or A_2MoO_4–MoO_3–MoO_2 melts) (10–12). The formation in our low temperature route proceeds in a solid-phase process different than those in the usual methods. We have been studying the low temperature route, expectig that it will provide industrial and/or scientific merits (handling easiness, formation of new types of metal bronzes, and so on) (7). So far, four kinds of cesium molybdenum bronzes have been known: (i) $Cs_{0.33}MoO_3$ [red, $a = 15.862$, $b = 7.728$, $c = 6.4080$ Å, and $\beta = 94.37^\circ$ (monoclinic, $C2/m$), characterized by infinite sheets composed of corner-sharing subunits of six edge-sharing MoO_6 octahedra (eclipsed hump-double chains)] (13), (ii) $Cs_{0.25}MoO_3$ [copper, $a = 6.425$, $b = 7.543$, $c = 8.169$ Å, and $\beta = 96.50^\circ$ (monoclinic, $P2_1/m$), infinite sheets composed of corner-sharing subunits of six edge-sharing MoO_6 octahedra (staggered hump-double chains)] (14), (iii) $Cs_{0.19}MoO_{2.85}$ (15) or $CsMo_{4-x}O_{12}$, ($x \simeq 0.13$) (16) [blackish-blue, $a = 19.063$, $b = 5.5827$, $c = 12.1147$ Å, and $\beta = 118.94^\circ$ (monoclinic, $C2/m$), infinite polyhedral sheets with corner-sharing MoO_4 tetrahedra and MoO_6 octahedra], and (iv) $Cs_{0.14}MoO_3$ [dark blue, $a = 10.620$, $c = 3.722$ Å (hexagonal, $P6_3/m$), hexagonal tungsten bronze type structure] (17). The low-temperature technique provided a new cesium molybdenum bronze, which was different than the above four types of Cs molybdenum bronzes, but was isostructural with the well known alkali metal bronze $A_{0.30}MoO_3$ (A = K, Rb, Tl, usually called 'blue bronze') (18–21). Recently, the Manthiram group has reported another low-temperature route for the preparation of alkali metal molybdenum bronzes

0022-4596/98 $25.00

(22). However, they have never reported the formation of new alkali metal bronzes.

In this paper, we will report the interesting findings of Cs-Na ion exchange on the hydrated bronze and details of the formation of new cesium molybdenum bronze by our low-temperature route.

EXPERIMENTAL

Starting Material

The starting material for the ion exchange was prepared by the method of Thomas and McCarron (3), and its typical composition was $(Na \cdot nH_2O)_{0.25}H_{0.08-0.12}MoO_3$, $n = 2$ (vacuum dried [VD] type) or 5–6 (air-dried [AD] type).[2] In order to investigate the effects of the interlayer spacing size on the ion-exchange behavior, two types of starting materials with a different interlayer spacing (i.e., AD- and VD-type hydrated bronzes) were used.

Since the starting materials were partially protonated, deprotonated materials, which were obtained by treating the original materials suspended in water with bubbled O_2 gas, were also used. Various deprotonation conditions were tried, and the completely deprotonated sample was obtained by treating the material at 323 K for a week.

Ion-Exchange Procedure

In a typical ion-exchange procedure, 2 g of the starting material was suspended in 40 ml of 0.8 M cesium chloride solution at 303 K for 24 h. N_2 gas was bubbled through the suspension during the exchange. After the exchange, the sample was filtrated and washed wth water. The unwashed sample was also investigated to obtain reliable structural information on the sample in suspension, if necessary.

Heat-treatment in N_2 of the Ion-Exchanged Samples

The heat treatment of the samples was performed on a MAC Science TG-DTA system 2010 with 100 ml/min of N_2 flow. The sample was ground with a mortar and pestle, and placed in an Al or Pt cell, with 20–40 mg of sample treated per batch. Several batches of samples were collected, if necessary.

Measurements and Analyses

The structure of the sample was investigated using a RIGAKU RINT 1200 M diffractometer with Cu$K\alpha$ radiation (40 KV, 40 mA). In usual measurements the diffraction data were collected at 2θ intervals of 0.02° at a scanning rate of 3°/min. For precise measurements, the stepwise measurement with 2θ intervals of 0.002° and integration time of 1 s for each step was used. For identification, the XRD patterns were simulated using the Rietveld analysis program, RIETAN-94 (23, 24), if necessary. TG and DTA were performed on the TG-TDA unit mentioned above, at a heating rate of $10\,K \cdot min^{-1}$. The Na, Cs, and Mo contents of the samples were measured using a Hitachi atomic absorption spectrophotometer with the 5890.0 Å line of Na, the 8521.0 Å line of Cs, and the 3132.6 Å line of Mo, respectively. The Mo^{5+} content of the samples was determined by the method of Choain and Marion (25). The magnetic susceptibility of the sample was measured on a Quantum Design MPMS-2 SQUID magnetometer at 1 T of applied field. The sample was pressed into a pellet and placed in a plastic straw. The background caused by the straw was also measured and was used to correct susceptibility of the sample.

[2] The partially protonated compound was usually obtained according to the preparation method of Thomas and McCarron, even if the buffer was used to keep the solution neutral. We have already investigated why protons were inserted during the preparation. The results will be reported elsewhere.

RESULTS

Cs/Na Ion Exchange and Formation of Hydrated Cesium Molybdenum Bronze

Figure 1 shows the XRD patterns of the samples prepared by treating the AD-type hydrated sodium bronze (with a larger interlayer spacing, $d_{020} \cong 11.4$ Å) with the Cs chloride solution, varying the treatment time. This figure shows

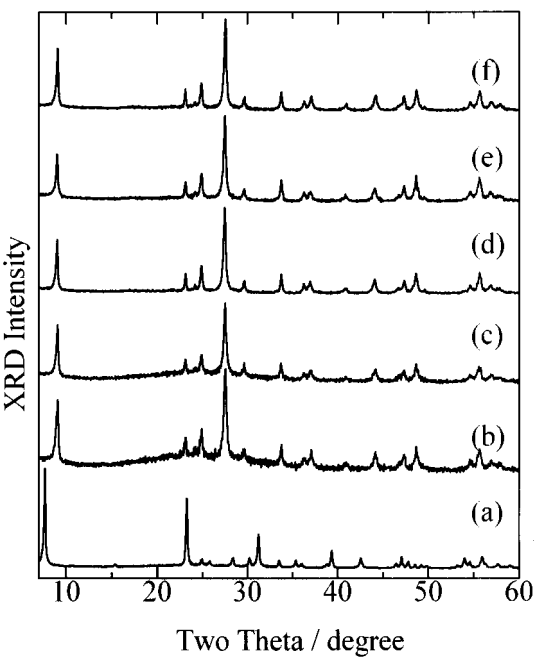

FIG 1. XRD patterns of (a) the hydrated Na bronze (AD type) and the samples ion-exchanged for various times: (b) 30 s, (c) 1 h, (d) 12 h, (e) 24 h, and (f) 48 h.

that 30 s of treatment time is sufficient for the sample to change its structure from the hydrated sodium bronze type to the hydrated Cs bronze type, and suggests that the ion exchange proceeds rapidly, similar to those of K/Na and Rb/Na (5, 6). However, according to the analysis of the samples' composition, the Cs/Na ion exchange was special. Figure 2 shows the changes in the alkali-metal contents of the sample with treatment time. About 0.05 alkali metal (A)/Mo of Na ion was left in the sample after 48 h of ion exchange treatment. Further ion-exchange procedure with fresh Cs chloride solution after the 48 h treatment did not reduce the Na content of the sample. These facts imply that the ion exchange is not achieved completely for this case, in contrast to the ion exchanges of K/Na and Rb/Na. The ion-exchanged sample initiated on the VD hydrated bronze (with a smaller interlayer spacing, $d_{020} \cong 9.7$ Å) had a higher Na content, as shown in Table 1, and it was suggested that the ion exchange of Cs/Na was prevented by the smaller interlayer spacing. Furthemore, after many efforts to improve the ion-exchange ratio, we found that proton contamination in the starting material prevented the complete Cs/Na ion exchange. Table 1 also shows a comparison between the samples initiated on a deprotonated Na molybdenum bronze and on the original hydrated Na bronze (treatment time = 24 h). The complete ion exchange was achieved on the starting material with no proton contamination, and the hydrated Cs bronze with the highest Cs content ($\sim$023 A/Mo) was obtained. We should note that

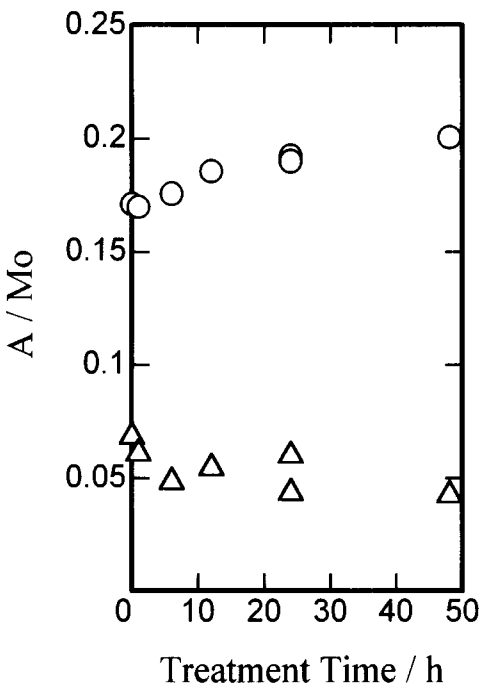

FIG. 2. The changes in alkali-metal contents for the sample with the treatment time. △ and ○ indicate Na and Cs contents, respectively.

TABLE 1
Chemical Compositions of the Samples Ion-Exchanged for 24 h

	Initial		Final		
Starting materials	Na/Mo	Mo^{5+}/Mo	Na/Mo	Cs/Mo	Mo^{5+}/Mo
AD original bronze	0.25	0.36	0.06	0.19	0.30
VD original bronze	0.25	0.36	0.14	0.10	0.27
AD deprotonated bronze	0.23	0.23	0.00	0.23	0.23

such contamination did not affect the ion exchange for K/Na and Rb/Na (4–6). Furthermore, we should mention that the hydrated Cs bronze shows different behavior than the other hydrated bronzes. So far, three types of hydrated bronze structure have been known (3): (i) AD-type structure, where the inserted alkali-metal ions are coordinated by only hydration water molecules, (ii) VD(6) structure, where the ions are six-coordinated by two hydration water molecules and four terminal oxygen ions of the host layer, and (iii) VD(8) structure, where the ions are eight-coordinated by terminal oxygen ions. The AD-type structure of the three has the largest interlayer spacing and is usually observed in the as-prepared sample. This type of bronze has been observed for Li, Na, K, and Rb (1, 3, 6), but was not found for hydrated Cs bronze, even in the wet as-prepared sample just after filtration.

Structural Changes by Heat Treatments of the Ion Exchanged Samples

The alkali metal bronze can be prepared by heat-treating the hydrated bronze in N_2. This synthesis route is expected to provide some merits, for example, in the preparation of any alkali metal bronze, as mentioned. Therefore, structural changes of the hydrated Cs bronze by heat-treatment in N_2 were investigated. TG and DTA curves in N_2 of the fully ion-exchanged sample with the composition $[Cs \cdot 0.7H_2O]_{0.23}MoO_3$ are shown in Fig. 3. This sample shows endothermic peaks below approximately 520 K with large weight loss, an exothermic peak at 623 K with no weight change, and endothermic peaks with no weight change near 800 K. The endothermic peaks below about 520 K are attributed to release of water from the sample,[3] while the endothermic peaks near 800 K are ascribed to the formation of melts. According to our experience, the exothermic peak seemed to result from the structural change from the hydrated bronze to an alkali metal bronze. And the weight loss above 900 K is ascribed to decomposition of the sample. Figure 4 shows the XRD patterns of the

[3] Grinding the sample tended to increase its water content. The increment seemed to be due to physisorption of water.

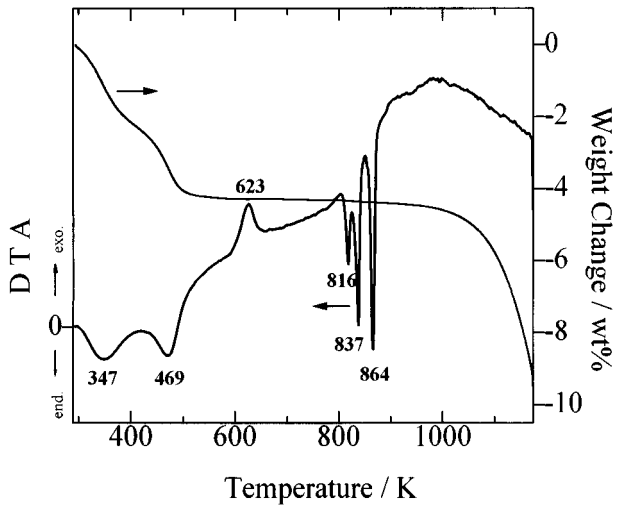

FIG. 3. TG-DTA curves in N_2 of the fully ion-exchanged, hydrated Cs bronze.

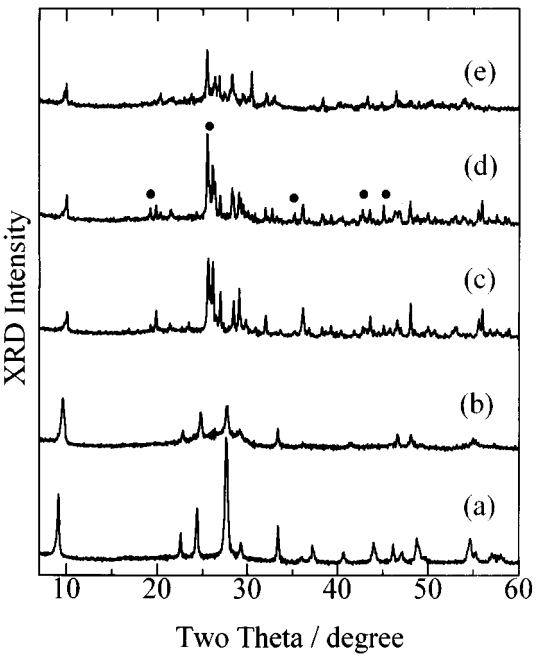

FIG. 4. The changes in XRD pattern of the fully ion-exchanged hydrated Cs bronze with the heat-treatment temperature: (a) no heat treatment, (b) 463 K, (c) 673 K, (d) 773 K, and (e) 973 K. ● indicates the peaks newly appeared in the temperature range 673–773 K.

fully ion-exchanged samples heat-treated in N_2 at various temperatures just before or just after the DTA peaks. The sample below the exothermic peak at 623 K maintained the hydrated Cs bronze structure (Figs. 4a and b), but a structural change is observed above 623 K (Fig. 4c). This structural change seemed to be due to the change from the hydrated bronze structure to alkali metal bronze structure, but the resultant XRD pattern could not be identified with any JCPDS data for the compounds composed of Mo, Cs and O. Details in identification of this phase will be given below in Discussion. A pattern similar to that of alkali decamolybdate, $A_2Mo_{10}O_{31}\cdot nH_2O$ (26), appeared in the range 673–773 K and is marked with symbol ● in the figure (Fig. 4d). This change was not associated with any obvious changes in TG and DTA curves. The heat treatment at 973 K (temperature above the melting point) resulted in some changes in the XRD pattern (Fig. 4c).[4]

Figure 5 shows a comparison betweeen the fully ion-exchanged and the Na-contaminated (prepared from the original hydrated sodium bronze with proton contamination) bronzes for the structure after the exothermic peak at about 620 K. This figure also shows the XRD pattern of the sample initiated on the original hydrated sodium bronze (Fig. 5c), which is mainly attributed to the purple sodium molybdenum bronze, $Na_{0.9}Mo_6O_{17}$. The incomplete ion-exchanged sample (with 0.06 Na/Mo and 0.19 Cs/Mo) showed some peaks due to $Na_{0.9}Mo_6O_{17}$ (Fig. 5b), indicating that the Na contamination resulted in the formation of $Na_{0.9}Mo_6O_{17}$. The lines, especially that at $2\theta = 23.1^\circ$, were rather large, although the Na content was not so large (the sample contained about 35 wt% of $Na_{0.9}Mo_6O_{17}$, if all Na ions in the sample were used to form $Na_{0.9}Mo_6O_{17}$). And the line at $2\theta = 23.1^\circ$ (indicated by a dotted line) could be used to check qualitatively whether the ion-exchange sample was contaminated by Na^+.

DISCUSSION

Cesium–Sodium Ion Exchange Behavior on the Hydrated Bronze

As mentioned above, the complete ion exchange of Cs/Na was prevented by protons in the intralayer sites, in contrast to the ion exchange of K/Na and Rb/Na. At first, the prevention of complete ion exchange seemed to result from the larger ionic radius of Cs, since a similar effect was seen in the case where hydrogen was inserted into alkali decamolybdates with large one-dimensional channels (tunnels) in their structure.[5] Figure 6 shows schematic models of the hydrated bronzes. The hydrated Cs bronze adopts only

[4] In the XRD pattern, the lines due to the decamolybdate-like phase disappeared (Figs. 4d and 4e). We think that some of the other changes in the XRD pattern are related to crystal growth in a particular direction during solidifying, but the resultant pattern has not been fully identified yet.

[5] Hydrogen insertion to alkali decamolybdate was prevented by large alkali ions in tunnel sites. This effect was suggested to result from the electrostatic repulsion between proton and alkali-metal ions. The details will be reported elsewhere.

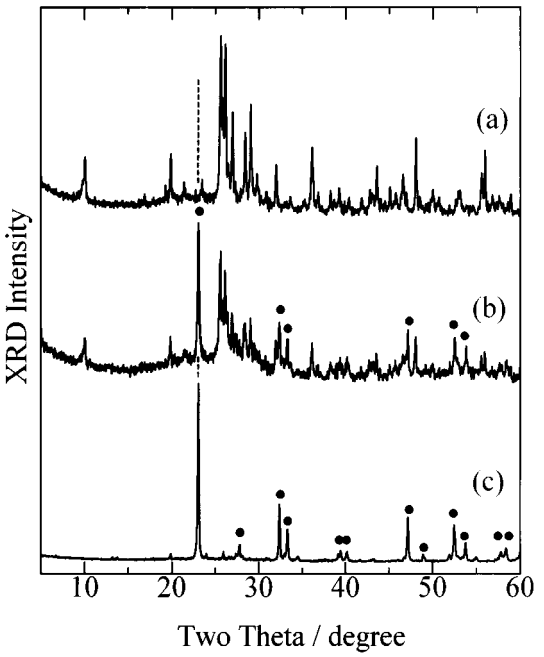

FIG. 5. The XRD patterns of the samples after the exothermic peak near 620 K initiated on (a) the fully ion-exchanged, hydrated Cs bronze, (b) the Na-contaminated, hydrated Cs bronze, and (c) the hydrated Na bronze. ● indicates the peaks of $Na_{0.9}Mo_6O_{17}$.

TABLE 2
Interlayer Spacing of the Hydrated Bronzes[a]

	Ionic radii[b]		AD		VD(6)		VD(8)	
Guest ion	$r(6)$	$r(8)$	d_{020}	spacing	d_{020}	spacing	d_{020}	spacing
Na	1.16	1.32	11.44	5.24	9.69	3.49	—	—
K	1.52	1.65	11.40	5.20	10.56	4.36	9.24	3.04
Rb	1.66	1.75	11.29	5.09	—	—	9.42	3.22
Cs	1.81	1.88	—	—	—	—	9.73	3.53

[a] The values are given in Å. Spacing is calculated by an equation, $d_{020} - 6.20$, where the value 6.20 is the thickness of the layer calculated from the atomic positions of terminal oxygen of the layer (27).

[b] r (6) and r (8) indicate ionic radii for six-coordination, and eight-coordination, respectively (28).

the VD(8) structure (Fig. 6c), and the prevention of complete ion exchange can be explained by the electrostatic repulsion between Cs^+ ions in the interlayer sites and protons (H^+) in the intralayer sites. As shown in Table 2, the interlayer spacing ('spacing' in the table) varies with the size of alkali-metal ion in the interlayer site for VD(8)-type bronzes, and this fact means that the separation between the alkali ion and proton in the intralayer site does not vary much with the size of the cation. So, the repulsion in the VD(8)-type hydrated bronzes of the other alkali metals (K, Rb) is

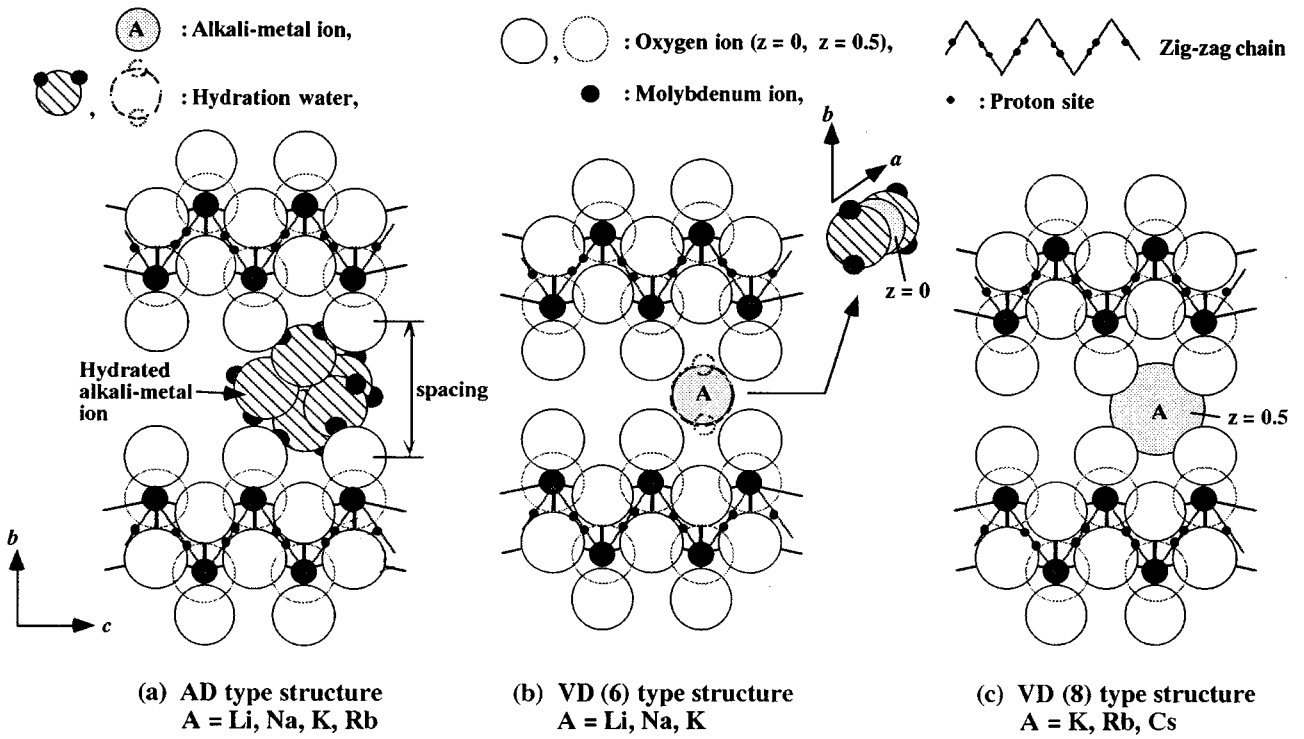

FIG. 6. Schematic models of the hydrated alkali metal bronzes. (a, b) were drawn for Na, while (c) for Cs. For the lattice constant c and atomic positions for Mo and O, the values obtained from the Rietveld analysis of powder neutron diffraction for the VD (6) type of hydrated Na bronze (27) were used in common, and for the basal spacing, d_{020}, the respective values in Table 2 were used. Oxygen and alkali-metal ions were expressed in a correct reducing scale using their ionic radii given in the literature (28).

expected to be similar. However, the complete ion exchange was observed for K/Na and Rb/Na ion exchanges with formation of VD(8)-type bronzes. For these two ion exchanges, the structure during the exchange process was usually the AD-type (Fig. 6a), where the repulsion was not likely to occur because of the hydration of the alkali-metal ion. Only for the ion exchange of Cs/Na, was the VD structure directly formed during the ion exchange process. Thus, we suggest that this difference in structure during the exchange process (i.e., the difference in hydration behavior of the bronze) resulted in the prevention of complete ion exchange only for the case of Cs/Na exchange.

Formation of New Cesium Molybdenum Bronze

To identify the phases formed by the heat treatment, we used the XRD pattern obtained by the precise measurement described above in Experimental. And, since JCPDS data are not available for all known compounds, we calculated the XRD patterns of all Cs molybdenum bronzes known so far using the crystal data from the literature in order to compare the XRD pattern of the present sample with them. Figure 7 shows a comparison of the observed XRD pattern with simulated ones. Although the XRD patterns of $Cs_{0.14}MoO_3$ and Cs-decamolybdate[6] are very similar, the XRD pattern of the phase in the sample appeared in the temperature range 673–773 K (cf., Figs 4c and d) and matched the XRD pattern of the decamolybdate better than that of $Cs_{0.14}MoO_3$ (Figs. 7a, b, and c). Thus, the phase was attributed to Cs-decamolybdate. The rest of the lines of the XRD pattern in Fig. 7a could be indexed by a monoclinic cell. The lattice parameters were $a = 19.362(8)$, $b = 7.567(2)$, $c = 10.506(4)$ Å, and $\beta = 121.07(3)^\circ$, based on a least-squares fit of 27 powder diffraction lines, which were not overlapped with those of Cs-decamolybdate, with $2\theta < 60^\circ$. These lattice parameters were similar to those of the blue alkali metal molybdenum bronze $A_{0.3}MoO_3$. The pattern for the blue bronze structure of Cs was simulated using the atomic positions of $K_{0.3}MoO_3$ (19).[7] The simulated pattern is shown in Fig. 7c, and agrees well with the observed one (Fig. 7a). Thus, the phase appearing with the exothermic peak at 623 K is suggested to have $A_{0.3}MoO_3$ type structure. This fact indicates the formation of new Cs molybdenum bronze, since the Cs analogue of $A_{0.3}MoO_3$ has not been found or has been known not to form. As the blue bronzes have been known to exhibit a metal-to-insulator transition (MIT) at about 180 K (29–31), the magnetic behavior of the sample in the temperature range where the MIT can be observed was also measured. The result is shown in Fig. 8, together with the literature data for $K_{0.3}MoO_3$. For the Cs sample as well as $K_{0.3}MoO_3$, the transition from paramagnetic to diamagnetic susceptibility is seen at about 180 K, indicating the MIT. This result also supported the formation of the blue bronze type phase.

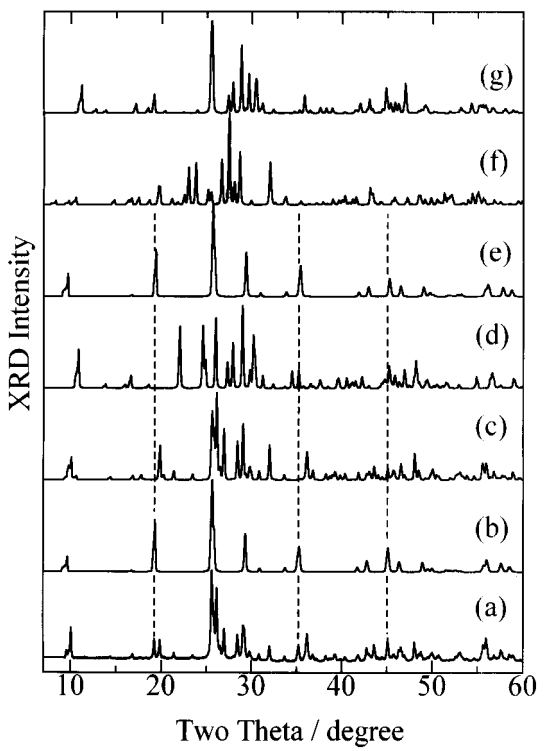

FIG. 7. XRD patterns: (a) observed pattern for the fully ion-exchanged bronze heated at 773 K in N_2, and simulated patterns (b) Cs decamolybdate, (c) Cs molybdenum bronze with $K_{0.3}MoO_3$-type structure, (d) $Cs_{0.25}MoO_3$, (e) $Cs_{0.14}MoO_3$, (f) $CsMo_{4-x}O_{12}$, and (g) $Cs_{0.33}MoO_3$.

CONCLUSION

In the present work, we investigated the ion-exchange behavior of hydrated molybdenum bronzes and revealed that the protons in the intralayer sites played an important role in the ion exchange of guest ions in the interlayer sites. This finding indicates that the introduction of protons becomes an effective modification of host structure, and it appears that such modification can be used to control the ion-exchange behavior of materials. Moreover, we found that our low-temperature route led to the formation of a new Cs molybdenum bronze which was isostructural with $A_{0.3}MoO_3$, A = K, Rb, Tl. The Cs analogue of the blue molybdenum bronzes could not be prepared previously by

[6] We determined the structural parameters of cesium decamolybdate with the composition $Cs_{0.17}Mo_{10}O_{30.85}\cdot 2.77H_2O$ by the Rietveld analysis of powder X-ray diffraction. The values were used for simulation. The structural data will be reported elsewhere.

[7] The atomic positions given in Ref. (19) were transformed to a $C2/m$ unit cell and used for the simulation. Since we never refined the atomic positions and so on, the calculated intensity cannot be related to the observed intensity exactly.

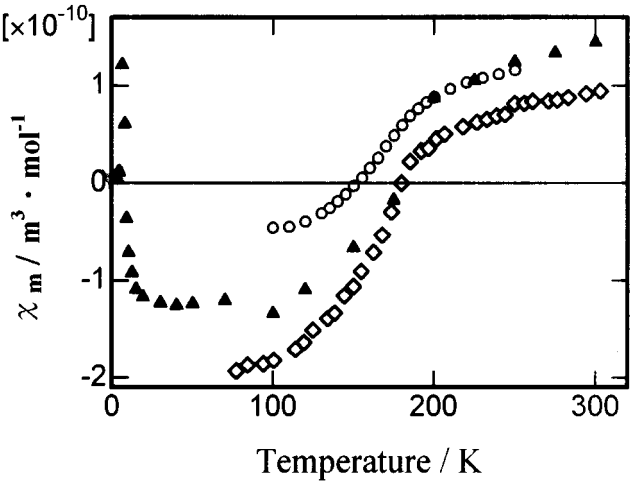

FIG. 8. Magnetic susceptibility of the samples: (○) for fully ion-exchanged, hydrated bronze heated at 773 K in N_2, (◇) for $K_{0.3}MoO_3$ (29), and (▲) for $K_{0.3}MoO_3$, (30). Diamagnetic contributions of the lattice and inserted alkali-metal ions were not subtracted.

conventional high-temperature techniques. Such low-temperature routes are likely to provide many opportunities for obtaining new materials.

The thermodynamical estimation of the effects due to the modification and preparation of single phase alkali-metal molybdenum bronzes by our synthesis route will be reported fully in the future.

REFERENCES

1. R. Schöllhorn, R. Kuhlmann, and J. O. Besenhard, *Mater. Res. Bull.* **11,** 83 (1976).
2. T. Iwamoto, Y. Itoh, K. Ohwaka, and M. Takahashi, *Nippon Kagaku Kaishi* **2,** 273 (1983).
3. D. M. Thomas and E, M, McCarron, III, *Mater. Res. Bull.* **21,** 945 (1986).
4. K. Eda, M. Suzuki, F. Hatayama, and N. Sotani, *J. Mater. Chem.* **7,** 821 (1997).
5. N. Sotani, T. Suzuki, K. Eda, M. Yanagi-ishi, and S. Takagi, *J. Solid State Chem.*, in press.
6. N. Sotani, T. Miyazaki, K. Eda, and F. Hatayama, *J. Mater. Chem.*, in press.
7. K. Eda, K. Furusawa, F. Hatayama, S. Takagi, and N. Sotani, *Mol. Cryst. Liq. Cryst.* **181,** 343 (1990).
8. K. Eda, K. Furusawa, F. Hatayama, S. Takagi, and N. Sotani, *Bull, Chem. Soc. Jpn.* **64,** 161 (1991).
9. N. Sotani, K. Eda, M. Yanagi-ishi, and S. Takagi, *Mater. Res. Bull.* **28,** 363 (1993).
10. J. M. Reau, C. Fouassier, C. Gleitzer, and M. Parmentier, *Bull. Soc. Chim. Fr.* 479 (1970).
11. A. Wold, W. Kunnmann, R. J. Arnott, and A. Fekrretti, *Inorg. Chem.* **3,** 545 (1964).
12. K. V. Ramanujachary, M. Greenblatt, and W. H. McCarroll, *J. Cryst. Growth* **70,** 476 (1984).
13. P. P. Tsai, J. A. Potenza, and M. Greenblatt, *J. Solid State Chem.* **69,** 329 (1987).
14. W. G. Mumme and J. A. Watts, *J. Solid State Chem.* **2,** 16 (1970).
15. L. F. Schneemeyer, S. E. Spengler, F. J. Disalvo, J. V. Waszczak, and C. E. Rice, *J. Solid State Chem.* **55,** 158 (1984).
16. S. C. Abrahams, P. Marsh, L. F. Schneemeyer, C. E. Rice, and S. E. Spengler, *J. Mater. Res.* **2,** 82 (1987).
17. L. E. Depero, M. Zocchi, F. Zocchi, and F. Demartin, *J. Solid State Chem.* **104,** 209–214 (1993).
18. J. Graham and A. D. Wadsley, *Acta Crystallogr.* **20,** 93 (1966).
19. M. Ghedira, J. Chenavas, M. Marezio, and J. Marcus, *J. Solid State Chem.* **57,** 300 (1985).
20. J. M. Reau, C. Fouassier, and P. Hagenmuller, *Bull. Soc. Chim. Fr.* 2883 (1971).
21. M. Ganne, A. Boumaza, M. Dion, and J. Dumas, *Mater. Res. Bull.* **20,** 1297 (1985).
22. C. Tsang, A. Dananjay, J. Kim, and A. Manthiram, *Inorg. Chem.* **35,** 504 (1996).
23. F. Izumi, *in* "The Rietveld Method" (R. A. Young, Ed.), Chap. 13. Oxford Univ. Press, Oxford, 1993.
24. F. Izumi, *J. Ceram. Soc. Jpn.* **102,** 401 (1994).
25. C. Choain and F. Marion, *Bull. Soc. Chim. Fr.* 212 (1963).
26. "Gmelin Handbook, Mo," Vol. B4, Springer-Verlag, Berlin, 1985.
27. K. Eda, M. Kunitomo, P. G. Dickens, and N. Sotani, *in* "International Chemical Congress of Pacific Basin Societies, Honolulu, December, 1995," Abstract Inor 051.
28. F. A. Cotton and G. Wilkinson, "Advanced Inorganic Chemistry," 5th ed., Wiley, New York, 1988.
29. B. L. Morris and A. Wold, *Rev. Scientific Instru.* **39,** 1937 (1968).
30. G. Bang and G. Sperlich, *Z. Phys. B. Condens. Matter* **22,** 1 (1975).
31. M. Greenblatt, *Chem. Rev.* **88,** 31 (1988), and references therein.